Computational stochastic heat transfer with model uncertainties in a plasterboard submitted to fire load and experimental validation

S. Sakji, Christian Soize, J.-V. Heck

Computational stochastic heat transfer with model uncertainties in a plasterboard submitted to fire load and experimental validation

S. Sakji[1], C. Soize[2*] & J.-V. Heck[3]

February 21, 2008

Abstract: The paper deals with probabilistic modeling of heat transfer throughout plasterboard plates when exposed to an equivalent ISO thermal load. The proposed model takes into account data and model uncertainties. This research addresses a general need to perform robust modeling of plasterboard-lined partition submitted to fire load. The first step of this work concerns the development of an experimental thermo physical identification data base for plasterboard. These experimental tests are carried out by the use of a bench test specially designed within the framework of this research. A computational heat transfer model is constructed using data from the literature and also the identified plasterboard thermophysical properties. The developed mean model constitutes the basis of the computational stochastic heat transfer model that has been constructed employing the nonparametric probabilistic approach. Numerical results are compared to the experimental ones.

Keywords: computational heat transfer modeling, uncertainties, probabilistic modeling, experiments.

1 Introduction

Large Light Partitions (LLP) of 10 meters height and more, are non-loadbearing structures made up of plasterboards screwed on both sides of a metal frame of various constructive configurations. Besides structural requirements such as the resistance to impact loading and collision loads [1], a light partition must satisfy various fire resistance criteria when subjected to full scale tests under the ISO 834 thermal loading curve [2]. This last requirement can not be met when the structure dimensions exceed those of the testing furnaces (up to 3 m). One way to circumvent the dimensional difficulty is to evaluate partition behavior by means of experiments and computational models.
The different steps and/or difficulties of such an approach consists of, (1) the choice of the computational heat transfer model to adopt, (2) the experimental identification of the thermophysical properties, (3) the validation of the computational model to predict the thermal response of the system and (4) the updating of the parameters if necessary. It is obvious that this procedure introduces errors and approximations in the different levels of the approach and then in the computational heat transfer (CHT) model. For the first level, the more simplifications one uses in the modeling (in order to make simulations reasonable), the more modeling errors are introduced. For the second level which concerns the experimental identification of the thermophysical properties, it is clear that the

[1]Assistant professor, Université Paris-Est, Laboratoire Modlisation et Simulation Multi Echelle, MSME FRE 3160, 5 bd Descartes, 77454, Marne-la-Vallee, France.

[2]Professor, Université Paris-Est, Laboratoire Modlisation et Simulation Multi Echelle, MSME FRE 3160, 5 bd Descartes, 77454, Marne-la-Vallee Cedex 2, France. E-mail: christian.soize@univ-paris-est.fr

[3]Research Engineer, Centre scientifique et technique de batiment, 84, Jean-Jaures, Champs sur marne, France.

errors increase with the number of constants used in the modeling and their level of complexity in the experimental characterization procedure. In order to take into account uncertainties induced by the errors introduced in the different levels, a probabilistic modeling of uncertainties can be introduced.

In this context, data uncertainties can be taken into account using a parametric probabilistic approach by modeling uncertain parameters with random variables or stochastic fields (see *e.g.* Shinozuka [3], Székely [4], [5], [6], [7], [8]). The modeling with stochastic fields of the boundary value problem parameters and their representation on the polynomial chaos have introduced the notion of the stochastic finite element method (see *e.g.* [9],[10], [11], [12], [13]). Recently, the nonparametric probabilistic approach which takes into account data and model uncertainties [14] has been developed and validated for many applications in structural dynamics of complex systems and vibroacoustics (see *e.g.* [15], [16], [17]). It is important to notice that, by construction, the parametric approach can not take into account model uncertainties.

A plasterboard (cardboard-plaster-cardboard (CPC) multilayer) gives a higher resistance to an LLP thanks to the important quantity of capillary and chemically bound water contained in the plaster (21% of its weight) [18]. An ideal modeling of an LLP subjected to ISO thermal load should be a thermo-hygro-chemico-mechanical modeling. The complexity of such an approach and the important number of parameters which has to be identified led us to choose a thermo-mechanical approach [19]. In this approach, the hydrous phase is implicitly taken into account in the model as well as in the experimental protocol. Indeed, the mechanical plasterboards properties are determined by submitting them to the same thermal time evolution law that a light partition would receive during a conventional fire resistance test. For this matter, a new thermal loading bench (TLB) is designed allowing a time evolution thermal load equivalent to the ISO834 function to be reproduced on CPC specimens and then one performs, "quickly", mechanical tests [20]. During ISO834 equivalent thermal loading, each CPC specimen is parallel to the heat source panel. This paper deals only with the heat transfer aspect and the development of a probabilistic CHT model of prediction for plasterboard submitted to fire load.

The outline of the paper is as follows. In Section 2, an overview of the literature about the thermo physical properties of plasterboard is presented. The principle and the use of the TLB is also briefly described. In Section 3, a mean computational heat transfer model for plasterboards submitted to fire load is constructed. Its numerical predictions are also compared to the reference experimental results presented in Section 2. In Section 4, a computational probabilistic heat transfer model is constructed on the basis of the mean CHT model. Its numerical results are presented in Section 5.

2 Experimental identification of the thermo-physical properties of the CPC

Thermophysical properties of plasterboards depend on the composition of the plaster and on the plasterboard manufacturing process. These two aspects induce a variability in the microstructure and in the quantity of free and bound water which causes a variability of the plasterboard fire resistance capability. The review of the literature concerning plasterboards' thermophysical properties affirms the above comments. Indeed, some authors such as Mehaffey [21], Axenenko [18], Thomas [22], were interested in modeling the heat transfer throughout an LLP and focus on identifying thermophysical properties of plasterboard. These experimental results show a relatively important difference from one author to another which make difficult the choice of parameters to be used in the modeling. Moreover, Mehaffey [21] highlights the impact of heat evolution rate on the apparent specific heat of plasterboards small specimens (10-30 mg) by identifying this property using a differential scanning calorimeter for two scanning rates 2 °C.min^{-1} and 20 °C.min^{-1} (Fig. 1).

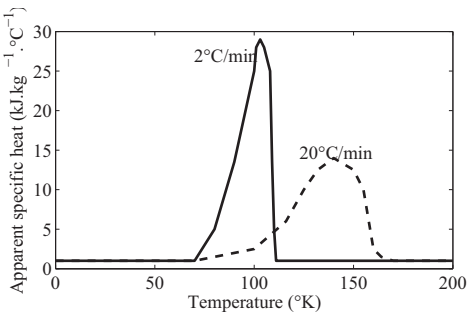

Figure 1: Impact of heat evolution rate on the apparent specific heat of plasterboards [21].

However, the actual thermal load in conventional fire resistance tests corresponds, at the exposed surface of an LLP, to a heat rate higher than 20 °C.min^{-1} till the first eight minutes of conventional tests. For this reason and taking into account previous remarks it turns out that it is worth trying to get indications about the plasterboard thermophysical properties according to a time evolution thermal load equivalent to that of the ISO 834 curve. In order to perform such tests we have used the experimental bench conceived and developed, within the framework of this research, to identify the thermo-mechanical characteristics of CPC plates. A brief description of this device is reported below.

2.1 Thermal load bench (TLB)

The TLB (See Fig. 2) reproduces an incidental heat flux equivalent to the one that a partition would receive during a mandatory test using a gas furnace. It is composed of a radiant panel (the heat source) and a mobile cart provided with a specimen holder. The heat flux received by the specimen, hung on the specimen holder, is modified by moving the cart with respect to the radiant panel. Hence, one can reproduce the ISO-thermal-load-equivalent heat flux, not by modifying the flow of combustible gas (as during tests on conventional furnaces (see *e.g.* [23])), but by modifying the distance between the specimen and the radiant panel. The specimen thermal loading takes place only when the radiant panel reaches its steady state. Therefore the emissive power can be considered as constant throughout the test duration. The combination of a heat source used in its steady state and a specimen movement controlled with a millimeter precision insures an excellent reproducibility of the thermal load. Furthermore, the use of a software [24] developed in order to model thermal exchanges in fire resistance furnaces, allows us to perform the calculation of the total heat flux received by the specimen surface at different time steps of conventional fire resistance test. First, one characterizes the incident heat flux received using a fluxmeter at different distances from the radiant panel and then, the cart displacement program is found out in order to reproduce by means of the TLB the incident heat flux calculated by the software. Figure 3 compares the proposed TLB heat flux with the calculated incident heat flux on the surface of a plasterboard specimen submitted to the ISO thermal load in a conventional furnace. It is to notice that during such tests only one side of the specimen is exposed to the heat source panel. Consequently, the direction of the heat flux and the hydrous transport are mainly transversal to the panel. Under these conditions, the assumption of a unidirectional heat transfer analysis throughout the thickness of the plasterboard is appropriate.

Figure 2: Thermal load bench composed of: ①: Specimen holder, ②: mobile cart and ③: radiant panel.

2.2 Thermophysical experimental identification

As mentioned previously the plasterboard thermophysical properties depend on thermal load evolution rate, it was then necessary, in order to be consistent with our approach, to identify the thermal conductivity and the diffusivity of the plasterboard according to ISO 834 thermal load. These tests were performed using the TLB (see Fig. 2). The thermal conductivity is determined by performing tests which consist on measuring, in the steady state conditions, the temperature at the heat exposed side and the unexposed side of plasterboard's specimens. Tests are performed for three different steps of thermal loading (3, 6 and 9 minutes of ISO thermal loading with the TLB). Knowing exactly the heat flux at the exposed side of the plasterboard (Fig. 3) we calculate the thermal conductivity. Figure 4 gives the thermal conductivity of the plasterboard BA13 for three different steps of thermal loading (marked points). According to the literature (*e.g* [22]) and the global shape of the thermal diffusivity (see Fig. 5), we determine an interpolation between the three points. The thermal dif-

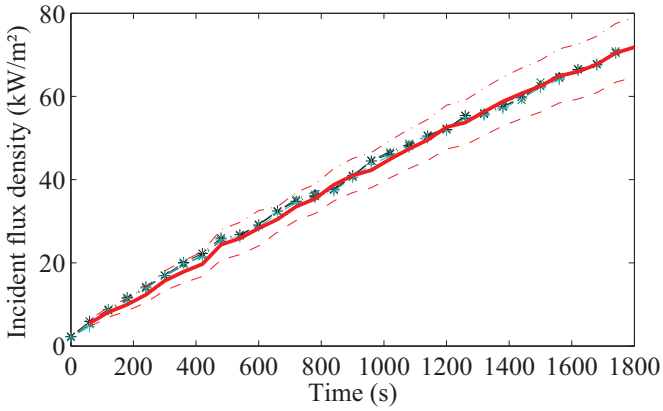

Figure 3: Heat flux (vertical axis in kW/m^2) as a function of time (horizontal axis in second): calculated heat flux (thick solid line), TLB measured heat flux (thin lines), upper and lower ISO 834 equivalent density flux bounds (dashed lines).

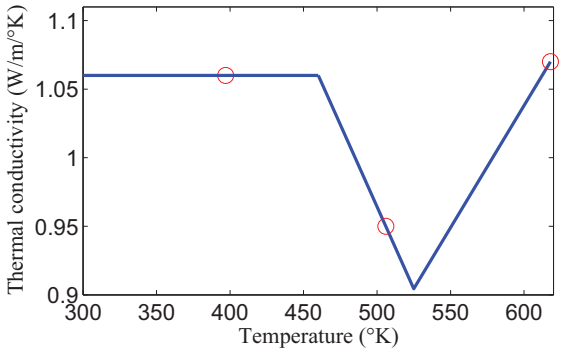

Figure 4: Thermal conductivity (vertical axis in W/m/K) as a function of temperature (◦K): measured conductivity (marks), interpolation (thin line).

fusivity (Fig. 5) is identified by solving an inverse problem for which the temperature is given at the exposed and the unexposed sides of plasterboard samples submitted to fire load using the TLB (Fig. 6). Figure 7 gives the comparison of these results with the reconstituted diffusivity using data collected from different authors (selected from literature see [21], [22]). It is clear that there is a shift of the first thermal diffusivity damping point when the thermal loading rate increases. This shift comes certainly from the shift of the specific heat (which is in agreement with Mehaffey's results (Fig. 1)). In order to update the CHT model prediction this remark is taken into consideration.

3 Mean computational heat transfer model

The usual finite element model for the nonlinear heat transfer analysis developed using the deterministic parameters is called the mean computational heat transfer (CHT) model. For a time duration t_{max}, the transient response $\{\mathbf{T}(t),\, t \in [0\,,\, t_{max}]\}$ of the mean CHT model satisfies the usual non linear time evolution problem,

$$[\underline{M}]\,\dot{\underline{\mathbf{T}}}(t) + [\underline{K}(\mathbf{T})]\,\underline{\mathbf{T}}(t) = \mathbf{f}(t) \quad , t \in [0\,,\, t_{max}] \quad , \tag{1}$$

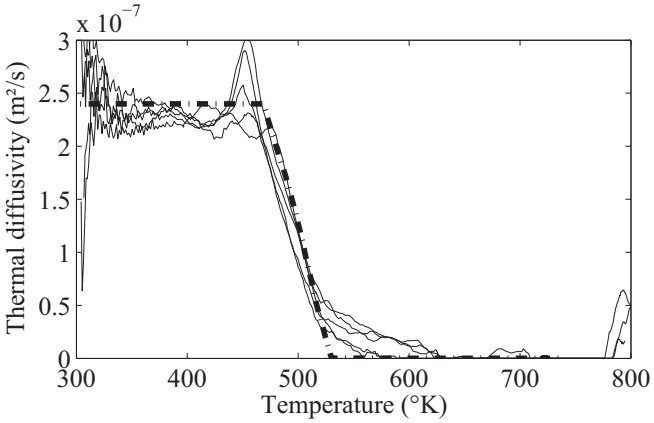

Figure 5: Thermal diffusivity of plasterboard as a function of temperature. Identified diffusivity (thin solid lines). Fitted diffusivity (thick dashed line).

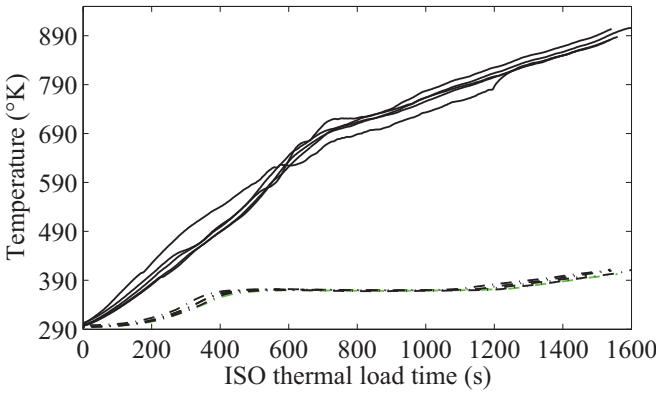

Figure 6: Thermal diffusivity tests performed on plasterboard. Temperature as a function of thermal loading time. Temperature measured at the heat exposed side (solid lines), temperature measured at the unexposed side of the plasterboard (dashed lines).

with $\underline{\mathbf{T}}(0) = \underline{\mathbf{T}}^0$. Matrices $[\underline{M}]$ and $[\underline{K}(\mathbf{T})]$ correspond to the global matrices constructed by the assembly of the elementary finite element matrices $[\underline{M}^e]$ and $[\underline{K}^e(\mathbf{T})]$ such that

$$[\underline{M}^e]_{ij} = \int_\Omega N_i^e \, N_j^e \, d\mathbf{x} \quad , \tag{2a}$$

$$[\underline{K}^e(\underline{\mathbf{T}})]_{ij} = \int_\Omega \nabla N_j^e \,.\, ([\underline{a}(\underline{T})] \nabla N_i^e) \, d\mathbf{x} + \int_{\Gamma_2} \frac{h_c}{\underline{\rho}(\underline{T}) \, \underline{c}(\underline{T})} \, N_i^e \, N_j^e \, ds \quad , \tag{2b}$$

where Ω is the domain and Γ_2 the part of its boundary which corresponds to the unexposed side of the plasterboard. Note that interpolation functions N^e of the finite element elementary domain Ω^e is zero if $\mathbf{x}$ does not belong to Ω^e. The term $\underline{\rho}(\underline{T})$ corresponds to the density and $[\underline{a}(\underline{T})]$ to the diffusivity matrix such that $[\underline{a}(\underline{T})] = [\underline{\lambda}(\underline{T})](\underline{\rho}(\underline{T}) \, \underline{c}(\underline{T}))^{-1}$, in which $[\underline{\lambda}(\underline{T})]$ is the thermal conductivity matrix, $\underline{c}(\underline{T})$ is the specific heat. The vector $\mathbf{f}(t)$ is constructed by the assembly of the elementary vectors $\mathbf{f}^e(\underline{\mathbf{T}})$ such that

$$\mathbf{f}_i^e(\underline{\mathbf{T}}) = \int_{\Gamma_2} \frac{h_c}{\underline{\rho}(\underline{T}) \, \underline{c}(\underline{T})} \, N_i^e \, T_{amb} \, ds \quad , \tag{3}$$

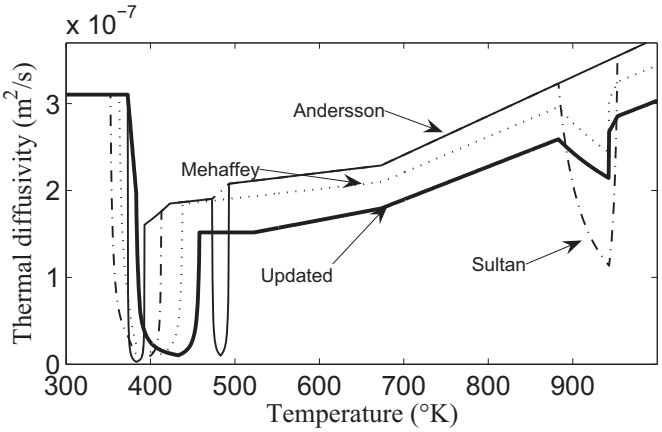

Figure 7: Reconstituted diffusivity according to different authors and the diffusivity used in the modeling (thick solid line).

where h_c is the convective heat transfer coefficient and T_{amb} is the room temperature. We introduce the time stepping $t_{n+1} = t_n + \Delta t$ for $n = 0, 1, 2, \ldots$ with $t_0 = 0$. The time discretization $t_{n+1} = \Delta t + t_n$ of Eq. (1) is performed using a central finite difference scheme which yields

$$[\underline{M}]\frac{\underline{\mathbf{T}}^{n+1,k} - \underline{\mathbf{T}}^{n}}{\Delta t} + [\underline{K}(\mathbf{T}^{n+1,k-1})]\frac{\underline{\mathbf{T}}^{n+1,k} + \underline{\mathbf{T}}^{n}}{2\Delta t} = \mathbf{f}^{n+1} \quad , n \geq 0 \quad , \tag{4}$$

in which the subscript k corresponds to internal iterations with $k \geq 1$ and where $\underline{\mathbf{T}}^{n+1,0} = \underline{\mathbf{T}}^{n}$. The convergence of the internal iterations is controlled by verifying the condition $\mid \underline{\mathbf{T}}^{n+1,k} - \underline{\mathbf{T}}^{n+1,k-1} \mid \leq \varepsilon \underline{\mathbf{T}}^{n+1,k}$. At convergence, we write $\underline{\mathbf{T}}^{n+1} = \underline{\mathbf{T}}^{n+1,k_{conv}}$ obtained for $k = k_{conv}$.

Mean model prediction

A finite element code is developed for the CHT model according to the scheme described by Eq. (4). The diffusivity implemented is the updated one given in Fig. 7. The implemented thermal conductivity is given by Fig .4. The heat convection coefficient is taken as 7 W/(m^2.K). Figure 8 shows the comparison of the numerical simulations output, using different authors' thermophysical identified properties and the updated one, with the experimental results (temperature at the unexposed side of plasterdoard's specimens submitted to fire load as a function of thermal loading time). A second study which correspond to the use of the identified thermophysical properties (Fig. 5) is considered (thick dashed line in Fig. 8). The two updated mean CHT models of prediction constitute the basis of the probabilistic model presented in the next section. In Fig. 8, temperature is in ($\circ$K) as a function of thermal loading time in (s). Mean updated model prediction is based on thermophysical properties selected from literature (thick solid curve), mean model prediction is based on identified thermophysical properties (thick dashed curve), measured temperature at the unexposed side (dashed lines). Model prediction according to Mehaffey's data (dot curves), Sultan's data (thin solid curve) and Andersson's data (dash-dot curve).

4 Computational stochastic heat transfer model

4.1 Data and modeling uncertainties

The sources of the data and model uncertainties are due to:

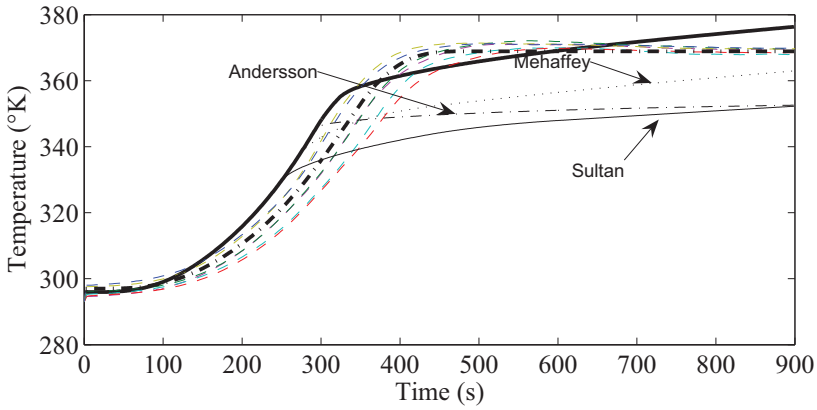

Figure 8: Mean model results compared to the temperature at the unexposed side of the plasterboard.

- thermo-physical properties: the diffusivity is assumed to be the same throughout the thickness of the plasterboard whereas it varies along the thickness of the plaster.
- the use of a simplified heat transfer model: in the proposed modeling the hydrous media is taken implicitly into account, whereas, in reality, the phenomenon is more complicated and should be modeled by a complete thermo-hygro-chemical model.
- the introduction of a one dimensional analysis.
- the variability of plasterboard composition.

Due to the presence of data and model uncertainties, a nonparametric probabilistic approach is adopted in order to take them into account.

4.2 Nonparametric probabilistic approach

According to the nonparametric probabilistic approach [14, 25], for a given vector $[\underline{\mathbf{T}}]$ of temperature, the matrices $[\underline{M}]$ and $[\underline{K}(\mathbf{T})]$ in Eq. (1) are replaced respectively by random matrices $[\mathbf{M}]$ and $[\mathbf{K}(\mathbf{T})]$ whose mean values are such that

$$\mathcal{E}\{[\mathbf{M}]\} = [\underline{M}] \in \mathbb{M}_n^+ \quad , \quad \mathcal{E}\{[\mathbf{K}(\mathbf{T})]\} = [\underline{K}(\mathbf{T})] \in \mathbb{M}_n^+ \text{ or } \in \mathbb{M}_n^{+0} \quad , \tag{5}$$

where $\mathcal{E}$ denotes the mathematical expectation, $\mathbb{M}_n^+$ denotes the set of positive-definite symmetric real matrices and $\mathbb{M}_n^{+0}$ denotes the set of positive symmetric real matrices. The probability density function of matrices $[\mathbf{M}]$ and $[\mathbf{K}(\mathbf{T})]$ are defined in the Sections 4.3 and 4.4 respectively. For all fixed time t, the deterministic unknown vector $\mathbf{T}(t)$ of temperature is no longer deterministic and becomes then a random vector $\mathbb{T}(t)$. Consequently, the family of random vectors $\{\mathbb{T}(t), t \in \mathbb{R}^+\}$ defines a stochastic process. For any fixed time t, random vectors $\mathbb{T}(t)$ and $\dot{\mathbb{T}}(t)$ verify the nonlinear stochastic differential equation,

$$[\mathbf{M}]\,\dot{\mathbb{T}}(t) + [\mathbf{K}(\mathbb{T}(t))]\,\mathbb{T}(t) = \mathbf{f}(t) \quad . \tag{6}$$

It can be verified (see e.g. [25]) that Eq. (6) has a second order solution ($i.e$, $\mathcal{E}\{\|\mathbb{T}(t))\|^2\} < +\infty\,, \forall t$) if

$$[\mathbf{M}] \in \mathrm{SE}^+ \quad , \tag{7}$$

and if, for every $\mathbf{T}$ fixed in $\mathbb{R}^n$,

$$[\mathbf{K}(\mathbf{T})] \in \mathrm{SE}^{+} \quad , \quad \text{when } [\underline{K}(\mathbf{T})] \in \mathbb{M}_n^{+} \quad , \tag{8}$$

or,

$$[\mathbf{K}(\mathbf{T})] \in \mathrm{SE}^{+0} \quad , \quad \text{when } [\underline{K}(\mathbf{T})] \in \mathbb{M}_n^{+0} \quad , \tag{9}$$

where SE^{+} denotes the set of all second-order random matrices with values in $\mathbb{M}^{+}(\mathbb{R})$ and SE^{+} set of all second-order random matrices with values in $\mathbb{M}^{+0}(\mathbb{R})$.

4.3 Probability density function of matrix [M]

The probability density function of the matrix $[\mathbf{M}]$ has values in SE^{+}. Under this condition, its probabilistic model is well defined (see e.g [14]) and it can be expressed as follows.
The mean value of random matrix $[\mathbf{M}]$ is equal to $[\underline{M}] \in \mathbb{M}_n^{+}(\mathbb{R})$ and can be written according

$$[\underline{M}] = [\underline{L}_M]^T [\underline{L}_M] \quad , \tag{10}$$

where $[\underline{L}_M]$ is a real upper triangular matrix. The random matrix $[\mathbf{M}]$ can be written such that

$$[\mathbf{M}] = [\underline{L}_M]^T [\mathbf{G}_M] [\underline{L}_M] \quad , \tag{11}$$

where $[\mathbf{G}_M]$ is a random matrix with values in $\mathbb{M}_n^{+}(\mathbb{R})$ and which the probability density function is expressed as a function of a unique dispersion parameter δ_M,

$$p_{[\mathbf{G}_M]}([G_M]) = \mathbb{1}_{\mathbb{M}_n^{+}\left(\mathbb{R}\right)}([G_M]) \times c_{G_M} \times (\det[G_M])^{(n+1)\frac{1-\delta_M^2}{2\delta_M^2}} \times \exp\left(-\frac{(n+1)}{2\delta_M^2} tr[G_M]\right) \quad , \tag{12}$$

in which the normalization positive constant c_{G_M} is written such

$$c_{G_M} = \frac{(2\pi)^{-n(n-1)/4} \left(\frac{n+1}{2\delta_M^2}\right)^{n(n+1)/(2\delta_M^2)}}{\left\{\prod_{\ell=1}^{n} \Gamma\left(\frac{n+1}{2\delta_M^2} + \frac{1-\ell}{2}\right)\right\}} \quad . \tag{13}$$

The dispersion parameter δ_M of the random matrix $[\mathbf{M}]$ is such that

$$\delta_M = \left\{ \frac{\mathcal{E}\{\|[\mathbf{G}_M] - [\underline{G}_M]\|_F^2\}}{\|[\underline{G}_M]\|_F^2} \right\}^{1/2} \quad , \tag{14}$$

and must be such

$$0 < \delta_M < \sqrt{\frac{n+1}{n+5}} \quad . \tag{15}$$

4.4 Probability density function of random matrix $[\mathbf{K}(\mathbb{T}(t))]$

For each temperature vector $\mathbf{T}$ fixed in $\mathbb{R}^n$, two cases can be met: either matrix $[\underline{K}(\mathbf{T})]$ of the mean model belongs to $\mathbb{M}_n^{+}(\mathbb{R})$, or it belongs to $\mathbb{M}_n^{+0}(\mathbb{R})$. The two cases studied correspond to taking or not convective heat flux boundary condition on the unexposed face of plasterboard's specimens. In the first case, matrix $[\underline{K}(\mathbf{T})]$ is definite-positive whereas in the second one it is only positive and its range is $m = n - 1$ for every temperature $\mathbf{T}$.
Case 1: convective boundary condition at the unexposed face. According to Eq. (8), for all temperature field $\mathbf{T}$ with values in $\mathbb{R}^n$, random matrix $[\mathbf{K}(\mathbf{T})]$ has values in SE^{+}. In this condition, its probabilistic

model is well defined (see [14]). The mean value of the random matrix $[\mathbf{K}(\mathbf{T})]$ given by Eq. (5) is equal to $[\underline{K}(\mathbf{T})] \in \mathbb{M}_n^+$ and can be written then according

$$[\underline{K}(\mathbf{T})] = [\underline{L}_K(\mathbf{T})]^T [\underline{L}_K(\mathbf{T})] \quad , \tag{16}$$

where $\mathbf{T} \mapsto [\underline{L}_K(\mathbf{T})]$ is a function with values in the set of the upper triangular matrices in $\mathbb{M}_n(\mathbb{R})$, it is constructed from the function $\mathbf{T} \mapsto [\underline{K}(\mathbf{T})]$.
Case 2: without convective boundary condition at the unexposed face. According to Eq. (9), for all temperature field $\mathbf{T}$ fixed in $\mathbb{R}^n$, random matrix $[\mathbf{K}(\mathbf{T})]$ have to be with values in the set SE^{+0}. In this condition, its probabilistic model is well defined (see [14]). The mean value of the random matrix $[\mathbf{K}(\mathbf{T})]$, given by Eq. (5), is equal to $[\underline{K}(\mathbf{T})] \in \mathbb{M}_n^{+0}$ and can be written then according

$$[\underline{K}(\mathbf{T})] = [\underline{L}_K(\mathbf{T})]^T [\underline{L}_K(\mathbf{T})] \quad , \tag{17}$$

where $\mathbf{T} \mapsto [\underline{L}_K(\mathbf{T})]$ is a function with values in the set of rectangular matrix $\mathbb{M}_{m,n}(\mathbb{R})$, which is constructed from the knowledge of the function $\mathbf{T} \mapsto [\underline{K}(\mathbf{T})]$.
Construction of the random matrix $[\mathbf{K}(\mathbf{T})]$. For all temperature field $\mathbf{T}$ fixed in $\mathbb{R}^n$, the random matrix $[\mathbf{K}(\mathbf{T})]$ is defined by

$$[\mathbf{K}(\mathbf{T})] = [\underline{L}_K(\mathbf{T})]^T [\mathbf{G}_K] [\underline{L}_K(\mathbf{T})] \quad , \tag{18}$$

where $[\mathbf{G}_K]$ is a random matrix with values in $\mathbb{M}_m^+(\mathbb{R})$ which the probability density function is defined by Eq. (19). Obviously it is clear that $m = n$ for the first case and $m = n - 1$ in the second one. The probability density function of the matrix $[\mathbf{K}(\mathbf{T})]$ is expressed as a function of the dispersion parameter δ_K according

$$p_{[\mathbf{G}_K]}([G_K]) = \mathbb{1}_{\mathbb{M}_m^+(\mathbb{R})}([G_K]) \times c_{G_K} \times (\det[G_K])^{(m+1)\frac{1-\delta_K^2}{2\delta_K^2}} \times \exp\left(-\frac{(m+1)}{2\delta_K^2} tr[G_K]\right) \quad , \tag{19}$$

where c_{G_K} is a positive variable such that

$$c_{G_K} = \frac{(2\pi)^{-m(m-1)/4} \left(\frac{m+1}{2\delta_K^2}\right)^{m(m+1)/(2\delta_K^2)}}{\left\{\prod_{\ell=1}^m \Gamma\left(\frac{m+1}{2\delta_K^2} + \frac{1-\ell}{2}\right)\right\}} \quad . \tag{20}$$

The dispersion parameter δ_K of the random matrix $[\mathbf{K}(\mathbf{T})]$ is independent of $\mathbf{T}$ and is such that,

$$\delta_K = \left\{\frac{\mathcal{E}\{\|[\mathbf{G}_K] - [\underline{G}_K]\|_F^2\}}{\|[\underline{G}_K]\|_F^2}\right\}^{1/2} \quad , \tag{21}$$

and must verify the condition

$$0 < \delta_K < \sqrt{\frac{m+1}{m+5}} \quad . \tag{22}$$

Construction of the random matrix $[\mathbf{K}(\mathbb{T}(t))]$. When the temperature vector describes the vectorial stochastic process $\mathbb{T}$, for each fixed t, $\mathbb{T}(t)$ describe a random vector and the the probabilistic vector of the random matrix $[\mathbf{K}(\mathbb{T}(t))]$ is

$$[\mathbf{K}(\mathbb{T}(t))] = [\underline{L}_K(\mathbb{T}(t))]^T [\mathbf{G}_K] [\underline{L}_K(\mathbb{T}(t))] \quad , \tag{23}$$

where $[\mathbf{G}_K]$ is the random matrix defined previously.

4.5 Generator of random germ matrices

For the Monte-Carlo simulation method, independent realizations of random matrices $[\mathbf{G}_K]$ and $[\mathbf{G}_M]$ (or random germs) are constructed using the following algebraic representation. Let $[\mathbf{A}]$ be a random matrix with values in $\mathbb{M}_n^+(\mathbb{R})$ which represents the random matrix $[\mathbf{M}]$ or $[\mathbf{K}]$. The random germ of the matrix $[\mathbf{A}]$ can be written according,

$$[\mathbf{G}_A] = [\mathbf{L}]^T[\mathbf{L}] \quad , \tag{24}$$

where $[\mathbf{L}]$ is an upper random triangular matrix such that,

- Random variables $\{[\mathbf{L}]_{kk'}, \quad k \leq k'\}$ are independent,
- For $\ell \leq \ell'$, the random variable $[\mathbf{L}]_{\ell\ell'}$, is such $[\mathbf{L}]_{\ell\ell'} = \sigma Y_{\ell\ell'}$, in which $\sigma = \delta/\sqrt{n+1}$ and $Y_{\ell\ell'}$ is a normalized Gaussian random variable,
- For $\ell = \ell'$, $[\mathbf{L}]_{\ell\ell} = \sigma\sqrt{2V_\ell}$ where V_ℓ is a gamma random variable which probability density function is given by

$$p_{V_\ell}(\nu) = \mathbb{1}_{\mathbb{R}^+}(\nu) \frac{1}{\Gamma\left(\frac{n+1}{2\delta_A^2} + \frac{1-\ell}{2}\right)} \nu^{\left(\frac{n+1}{2\delta_A^2} + \frac{1-\ell}{2}\right)} \exp^{-\nu} \quad . \tag{25}$$

5 Finite element discretization of the stochastic boundary value problem

The nonlinear boundary value problem of heat transfer analysis is approximated by the stochastic finite element method according to Eq. (6).

5.1 Stochastic solver

The Monte-Carlo simulation method is used as the stochastic solver for the nonlinear stochastic equation defined by Eq. (6). For a realization r_ℓ, the realization $\{\mathbb{T}^n(r_\ell),\, n \geq 1\}$ of the temperature random vector is given by solving the Eq. (6) according to the scheme (*see* Eq. (4)),

$$[\mathbf{M}(r_\ell)] \frac{\mathbb{T}^{n+1,k}(r_\ell) - \mathbb{T}^n(r_\ell)}{\Delta t} + [\mathbf{K}(\mathbb{T}^{n+1,k-1}(r_\ell), r_\ell)] \frac{\mathbb{T}^{n+1,k}(r_\ell) + \mathbb{T}^n(r_\ell)}{2\Delta t} = \mathbf{f}^{n+1},\ n \geq 0, \tag{26}$$

for $k \geq 1$ and $\mathbb{T}^{n+1,0}(r_\ell) = \mathbb{T}^n(r_\ell)$. The convergence of the internal iterations is controlled by verifying the condition $\mid \mathbb{T}^{n+1,k}(r_\ell) - \mathbb{T}^{n+1,k-1}(r_\ell) \mid \leq \varepsilon \mathbb{T}^{n+1,k}(r_\ell)$. At convergence (obtained for $k = k_{conv}$), we write $\mathbb{T}^{n+1}(r_\ell) = \mathbb{T}^{n+1,k_{conv}}(r_\ell)$ in which $\mathbb{T}^{n+1}(r_\ell) = \mathbb{T}(t_{n+1},\, r_\ell)$. The realization of the random matrices $[\mathbf{M}(r_\ell)]$ and $[\mathbf{K}(\mathbf{T}, r_\ell)]$ are constructed according to Eq. (11) and Eq. (17) respectively.

5.2 Confidence region estimator and stochastic convergence

For each time t, the confidence region is constructed for a given component $\mathbb{T}_j(t)$ of the random response temperature vector $\mathbb{T}(t)$. For a given probability P_c, the confidence region is defined by the upper and the lower bounds ($\tau^+(t)$ and $\tau^-(t)$ respectively) such as

$$\mathrm{Prob}(\tau^-(t) < \mathbb{T}_j(t) \leq \tau^+(t)) = \mathrm{P}_c \quad . \tag{27}$$

In order to simplify notations, t is omitted below. Let $T_1 = \mathbb{T}_j(r_1), \ldots, T_{n_s} = \mathbb{T}_j(r_{n_s})$ be n_s independent realizations of the random variable $\mathbb{T}_j$. Let $\widehat{T}_1 < \ldots < \widehat{T}_{n_s}$ be the order statistics of the independent variables $T_1, \ldots, T_{n_s}$. Therefore, a possible estimation of τ^- and τ^+ is

$$\tau^- \simeq \widehat{T}_{j^-} \text{ with } j^- = fix(n_s(1-P_c)/2) \quad , \tag{28a}$$

$$\tau^+ \simeq \widehat{T}_{j^+} \text{ with } j^+ = fix(n_s(1+P_c)/2) \quad , \tag{28b}$$

where $fix(x)$ is the integer part of the real number x. The convergence for an observed component of the stochastic temperature (subscript $jobs$) with respect to the number n_s of realizations $r_1, \ldots, r_{n_s}$ used in the Monte Carlo simulation is studied by analyzing the function

$$n_s \mapsto conv(n_s) = \left\{ \frac{1}{n_s} \sum_{\ell=1}^{n_s} \sum_{n>0} |\mathbb{T}^n_{jobs}(r_\ell)|^2 \right\}^{1/2} \quad . \tag{29}$$

5.3 Experimental identification of the probabilistic model dispersion parameters

When the mean model is in a reasonable agreement with the experimental average responses, the identification of the two dispersion parameters δ_K and δ_M with respect to the experimental dispersion δ^{exp} can be performed by minimizing the objective function defined by

$$J(\delta_M, \delta_K) = \{\delta^{mod}_{\widetilde{\nu}}(\delta_M, \delta_K) - \delta^{exp}_{\nu}\}^2 \tag{30}$$

under the constraints defined by Eq. (15) and Eq. (22). In Eq. (30), $\delta^{mod}_{\widetilde{\nu}}(\delta_M, \delta_K)$ and δ^{exp}_{ν} correspond to an estimation of the modeling and the experimental dispersions. The estimations are written as

$$\delta^{mod}_{\widetilde{\nu}}(\delta_M, \delta_K) = \frac{1}{\|\widehat{\mathbf{m}}^{mod}_{\widetilde{\nu}}(\delta_M, \delta_K)\|} \left\{ \frac{1}{\widetilde{\nu}} \sum_{\ell=1}^{\widetilde{\nu}} \|\mathbf{T}^{mod}_{\partial\Omega}(r_\ell, \delta_M, \delta_K) - \widehat{\mathbf{m}}^{mod}_{\widetilde{\nu}}(\delta_M, \delta_K)\|^2 \right\}^{1/2} , \tag{31a}$$

$$\delta^{exp}_{\nu} = \frac{1}{\|\widehat{\mathbf{m}}^{exp}_{\nu}\|} \left\{ \frac{1}{\nu} \sum_{\ell=1}^{\nu} \|\mathbf{T}^{exp}_{\partial\Omega}(\tau_\nu) - \widehat{\mathbf{m}}^{exp}_{\nu}\|^2 \right\}^{1/2} \quad . \tag{31b}$$

in which $\mathbf{T}^{mod}_{\partial\Omega}(r_1, \delta_M, \delta_K), \ldots, \mathbf{T}^{mod}_{\partial\Omega}(r_{\widetilde{\nu}}, \delta_M, \delta_K)$ are $\widetilde{\nu}$ independent realizations of the random variable $\mathbf{T}^{mod}_{\partial\Omega}(\delta_M, \delta_K)$ and where $\mathbf{T}^{exp}_{\partial\Omega}(\tau_1), \ldots \mathbf{T}^{exp}_{\partial\Omega}(\tau_\nu)$ are ν independent realizations of the random variable $\mathbf{T}^{exp}_{\partial\Omega}$. In Eq. (31.a) and (31.b), the estimations of the mean value of $\mathbf{T}^{mod}_{\partial\Omega}(\delta_M, \delta_K)$ and of the mean value of $\mathbf{T}^{exp}_{\partial\Omega}$ are written as

$$\widehat{\mathbf{m}}^{exp}_{\nu} = \frac{1}{\nu} \sum_{\ell=1}^{\nu} \mathbf{T}^{exp}_{\partial\Omega}(r_\ell) \quad , \tag{32}$$

$$\widehat{\mathbf{m}}^{mod}_{\widetilde{\nu}}(\delta_M, \delta_K) = \frac{1}{\widetilde{\nu}} \sum_{\ell=1}^{\widetilde{\nu}} \mathbf{T}^{mod}_{\partial\Omega}(r_\ell, \delta_M, \delta_K) \quad . \tag{33}$$

5.4 Probabilistic model prediction and experimental comparisons

We consider the boundary value problem corresponding to a heat transfer analysis throughout a plasterboard and which is discretized using the stochastic finite element method. We are interested in the random response $\mathbb{T}_{jobs}$ of the temperature at the unexposed side of the plasterboard as a function of the thermal loading time. The correspondence between the thermal loading time and the heat load

at the exposed side is easy to perform. Two analyses are considered, the first one corresponds to the computational stochastic heat transfer (CSHT) model constructed using the mean CHT model where the implemented parameters are given according to the updated data from the literature (thick solid curve in Fig 8). The second analysis corresponds to the CSHT model constructed around the mean CHT model (thick dashed curve in Fig. (8)) where the measured thermal diffusivity (thick dashed curve in Fig. (5)) and thermal conductivity (Fig. (4)) are used.

5.4.1 Case 1

The dispersion parameters δ_M and δ_K of the random matrices $[\mathbf{M}]$ and $[\mathbf{K}(\mathbf{T})]$ are identified with the experimental data using the random response $\mathbb{T}_{jobs}$ of the temperature at the unexposed side. Parametric analysis has been performed for (δ_M, δ_K) taking their values in $\{0.1, 0.12, 0.14, \ldots, 0.56, 0.58, 0.6\} \times \{0.1, 0.12, 0.14, \ldots, 0.56, 0.58, 0.6\}$. For each value of the dispersion parameters, the Monte Carlo simulation method is carried out with $n_s = 1200$ simulations. Figure 9 displays the graph of $n_s \mapsto conv(n_s)$ related to the convergence of the stochastic heat transfer model output. It can be seen that for $n_s = 700$ simulations, the solution of the stochastic model of the heat transfer analysis verifies the second-order convergence defined by Eq. (29). An "optimal" value of δ_M and δ_K has been determined in the time interval $[0, 350]s$, the lower envelope of the confidence region being close to the minimum values of the experiments. We have then obtained $\delta_M = 0.25$ and $\delta_K = 0.4$. Figure 10 displays the comparison of the experiments with the confidence region calculated according to Eq. (27) with $\mathrm{P}_c = 0.95$ and for $\delta_M = 0.25$ and $\delta_K = 0.4$. The estimation of the probability density function of the random variable $\mathbb{T}_{jobs}$ of the temperature at the unexposed side at observation time $t = 900s$ is given in Fig. 11.

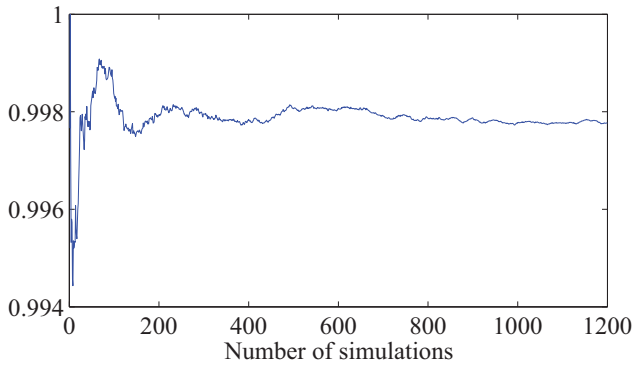

Figure 9: Convergence with respect to the number n_s of simulations: graph of function $n_s \mapsto conv(n_s)$.

5.4.2 Case 2

The dispersion parameters δ_M and δ_K of the random matrices $[\mathbf{M}]$ and $[\mathbf{K}(\mathbf{T})]$ are identified with the experimental data using the random response $t \mapsto \mathbb{T}_{jobs}(t)$ of the temperature at the unexposed side. Figure 12 shows the interpolated meshgrid within the calculated values of the objective function defined by Eq. (30). The minimum value of the objective function is obtained for $\delta_M = 0.03$ and $\delta_K = 0.35$. For the two fixed dispersion parameters, the Monte Carlo simulation method is carried out for n_s simulations with $n_s = 2000$. Figure 13 displays the graph of $n_s \mapsto conv(n_s)$ related to the convergence of the stochastic heat transfer model output (second-order convergence is obtained

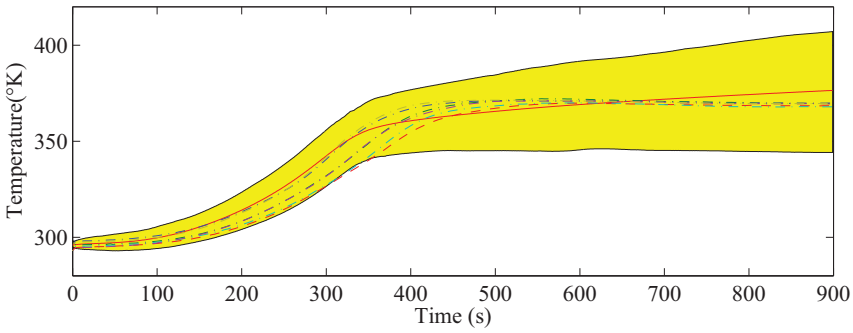

Figure 10: Prediction of the probabilistic CHT model for the dispersion parameters $\delta_M = 0.22$ and $\delta_K = 0.4$. Vertical axis: temperature at the unexposed side in °K as a function of thermal load time (s) (horizontal axis). Temperature measured on the unexposed side (dashed thin lines). Prediction of the mean model (thick solid line). Confidance region of the probabilistic model of heat transfer analysis for Pc=0.95: (grey zone).

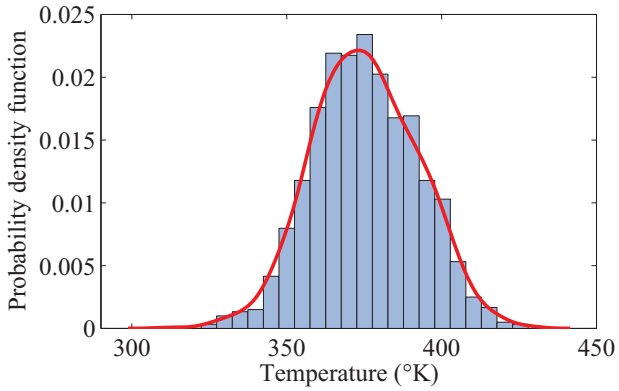

Figure 11: Graph of the probability density function of the temperature at the unexposed side of the plasterboard at t=900 s.

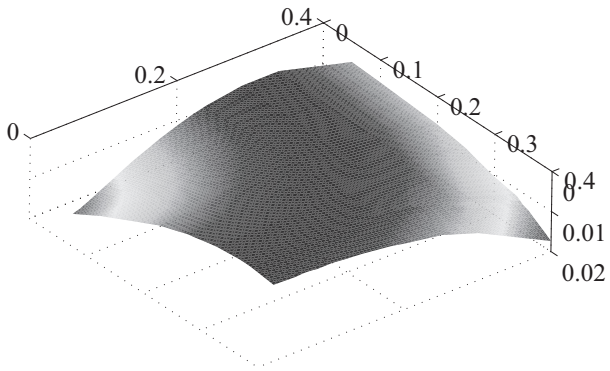

Figure 12: Graph of the objective function $(\delta_M, \delta_K) \mapsto J(\delta_M, \delta_K)$.

for $n_s = 1000$). Figure 14 displays the comparison of the experiments with the confidence region calculated according to Eq. (27). This result shows that even if the mean model gives a good

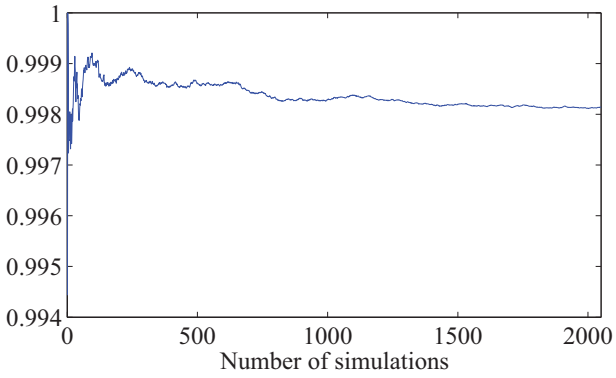

Figure 13: Convergence with respect to the number n_s of simulations: graph of function $n_s \mapsto conv(n_s)$.

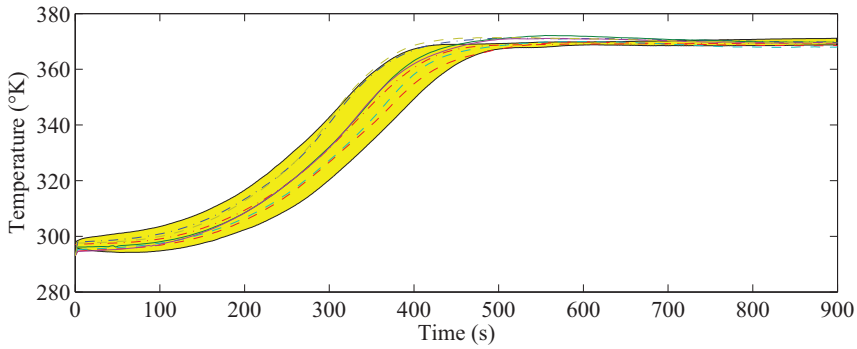

Figure 14: Prediction of the probabilistic CHT model for the dispersion parameters $\delta_M = 0.03$ and $\delta_K = 0.35$. Vertical axis: temperature at the unexposed side in °K (axe vertical) as a function of thermal load time (s) (horizontal axis). Experiments (dashed thin lines). Prediction of the mean model: thick solid line. Confidance region of the probabilistic model of heat transfer analysis for Pc=0.95 (grey zone).

prediction of the thermal behavior of the plasterboard, the probabilistic model is necessary to take into account the uncertainty induced firstly by errors in the modeling process and by the variability in thermophysical characteristics of the plasterboard samples (induced by the manufacturing process).

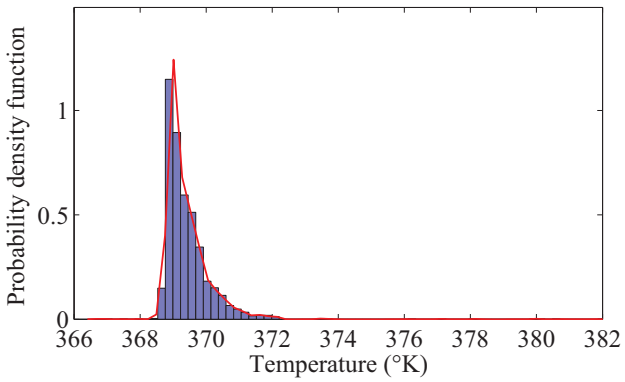

Figure 15: Graph of the probability density function of the temperature at the unexposed side of the plasterboard at t=900 s.

6 CONCLUSION

A deterministic and a probabilistic nonlinear heat transfer analysis throughout plasterboard have been presented. Note that a simplified model based on a nonlinear thermo-mechanical modeling has been used. This model could be improved by using a thermo-chemico-mechanical modeling. The main objective of this paper is to combine a probabilistic approach with the deterministic heat transfer analysis of plasterboards submitted to fire loads. Within the probabilistic model a confidence region can be constructed for the temperature according to the estimated dispersion parameters for a given probability level. The implemented nonparametric probabilistic approach allows two global dispersion parameters, which govern the heat transfer through a plasterboard submitted to fire load, to be identified. These two identified parameters, which take into account uncertainties induced by data and modeling errors, can be used as parametric probabilistic parameters in a general approach in order to model a large light partition.

Acknowledgement

The authors wish to acknowledge the support of the CSTB and the SNIP.

Notation

The following symbols are used in this paper:

CHT	Computational Heat Transfer;
CPC	Cardboard Plaster Cardboard;
$[\mathbf{G}_M]$, $[\mathbf{G}_K]$	random matrices germ related to the random matrices $[\mathbf{M}]$ and $[\mathbf{K}(\mathbf{T})]$;
h_c	convective heat transfer coefficient;
$[I]$	identity matrix;
ISO834	the ISO 834 curve;
LLP	Large Light partition;
TLB	Thermal Load Bench;
$[\underline{L}_S]$	real upper triangular matrix of cholesky decomposed matrix $[\underline{S}]$;
$[\underline{M}]$, $[\underline{K}]$	mean matrices of the deterministic CHT model;
$\mathbb{M}^+(\mathbb{R})$	set of positive-definite symmetric real matrices;
$\mathbb{M}^{+0}(\mathbb{R})$	set of positive symmetric real matrices;
n_s	number of simulations;
$P_c(X > x)$	probability that random variable X be greater than x;
r_ℓ	the ℓ^{th} realization belonging to the set of all the realizations;
SE^+	set of all second-order random matrices with values on $\mathbb{M}^+(\mathbb{R})$;
SE^{+0}	set of all second-order random matrices with values on $\mathbb{M}^{+0}(\mathbb{R})$;
$\mathbb{T}$	denotes the stochastic vector of temperature at the different nodes;
$\mathbf{T}$	denotes the deterministic vector of temperature at the different nodes;
$\underline{\mathbf{T}}$	vector of the mean temperature;
T_{amb}	denotes the room temperature;
$\mathbb{T}_{jobs}$	temperature at the observation point;
x	scalar variable;
$\mathbf{x}$	vector;
X	random variable associated to the scalar variable x;

$\mathbf{X}$	random vector associated to the vector $\mathbf{x}$;
$[\underline{S}]$	mean model matrix;
$[\mathbf{S}]$	random matrix;
$[S]^T$	transpose of matrix $[S]$;
$\|[S]\|_F$	Frobenius norm of matrix $[S]$ $\left(\|[S]\|_F = \text{tr}\ ([S][S]^T)^{1/2}\right)$;
$\text{tr}([S])$	trace of matrix $[S]$;
δ_K, δ_M	dispersion parameters of the random matrices $[\mathbf{M}]$ and $[\mathbf{K}(\mathbf{T})]$;
$\mathcal{E}\{\cdot\}$	mathematical expectation;
τ^-, τ^+	lower and upper envelopes of the confidence region;
$\mathbb{1}_{\mathbb{R}^+}(x)$	equal to 1 if $x \in \mathbb{R}^+$ and 0 elsewhere.

References

[1] European Commitee for Standardization. *Eurocode1: Basis of design and actions on structures, Part 2-2: Actions on structures exposed to fire, pp 20-23.*, 1994.

[2] ISO. *Fire Resistance Tests- Elements of Building Construction. International Standard ISO 834*, 1975.

[3] M. Shinozuka and C. J. Astill. Random eigenvalue problems in structural analysis. *AIAA Journal*, 10(4):456–462, 1972.

[4] G. S. Székely and G. I. Schueller. Computational procedure for a fast calculation of eigenvectors and eigenvalues of structures with random properties. *Computer Methods in Applied Mechanics and Engineering*, 191:799–816, 2001.

[5] G. I. Schueller, H. J. Pradlwarter, and C. A. Schenk. Nonstationnary response of large linear fe-models under stochastic loading. *Computers and Structures*, 81(8-11):937–947, 2003.

[6] M. Kleiber, D. H. Tran, and T. D. Hien. *The Stochastic finite Element Method*. New York: Jhon Wiley and Sons, 1992.

[7] T. D. Hien and M. Kleiber. Stochastic finite element modelling in linear transient heat transfer. *Computer Methods in Applied Mechanics and Engineering*, 144(1-2):111–124, May 1997.

[8] M. Kaminski and Hien T. D. Stochastic finite element modeling of transient heat transfer in layered composites. *International Communications in Heat and Mass Transfer*, 26(6):801–810, August 1999.

[9] E. Vanmarcke and M. Grigoriu. Stochastic finite element analysis of simple beams. *ASCE Journal of Engineering Mechanics*, 109(5):1203–1214, 1983.

[10] R. Ghanem. Stochastic finite elements with multiple random non gaussian properties. *Journal of Engineering Mechanics*, 125(1):26–40, 1999.

[11] C. Soize and R. Ghanem. Physical systems with random uncertainties: Chaos representation with arbitrary probability measure. *SIAM Journal on Scientific Computing*, 26(2):395–410, 2004.

[12] A. F. Emery. Solving stochastic heat transfer problems. *Engineering Analysis with Boundary Elements*, 28(3):279–291, March 2004.

[13] D. Xiu and Karniakadis G. E. A new stochastic approach to transient heat conduction modeling with uncertainty. *International Journal of Heat and Mass Transfer*, 46(24):4681–4693, November 2003.

[14] C. Soize. Random matrix theory for modeling uncertainties in computational mechanics. *Computer Methods in Applied Mechanics an Engineering*, 194(12-16):1333–1366, 2005.

[15] C. Desceliers, C. Soize, and S. Cambier. Nonparametric-parametric model for random uncertainties in nonlinear structural dynamics- application to earthquak engineering. *Earthquake Engineering and Structural Dynamics*, 33(3):315–327, 2004.

[16] E. Capiez-Lernout, C. Soize, J.-P. Lombard, C. Dupont, and E. Seinturier. Blade manufacturing tolerances definition for a mistuned industrial bladed disk. *Journal of Engineering for Gaz Turbines and Power*, 127(3):621–628, 2005.

[17] C. Chen, D. Duhamel, and C. Soize. Experimental identification and validation of a probability model addressing model uncertainties in structural dynamics: case of composite sandwich panels. *Journal of Sound and Vibration*, 294(1-2):64–81, 2006.

[18] O. Axenenko and G. Thrope. The modelling of dehydration and stress analysis of gypsum plasterboards exposed to fire. *Computational Materials Science*, 6:281–294, 1996.

[19] S. Sakji, C. Soize, and J.-V Heck. Thermo-mechanical modeling of plasterboard-lined partition submitted to fire load. In A.S.C.E, editor, *17th ACSE Analysis and Computation Speciality Conference, St Louis, USA*, 2006.

[20] S. Sakji, C. Soize, and J.-V Heck. Thermo-mechanical model of a cardboard-plaster-cardboard composite plate submitted to fire load and experiments. In UK C.A. BREBBIA, Wessex Institute of Technology and USA A.A. MAMMOLI, University of New Mexico, editors, *Computational Methods and Experiments in Material Characterisation II*, 2005.

[21] J.R. Mehaffey, P. Cuerrier, and Carisse G. A model for predicting heat transfer through gypsumboard/wood-stud wall exposed to fire. *Fire And Materials*, (18):297–305, 1994.

[22] G. Thomas. Thermal properties of gypsum plasterboard at high temperatures. *Fire and Materials*, (26):37–45, 2002.

[23] Ph. Fromy, M. Curtat, and D. Pardon. Note on the modelling of heat transfer in furnaces of fire resistance testing. Technical report, CSTB, 1995.

[24] Ph. Fromy and M. Curtat. Heat transfer in fire resistance furnaces piloted with thermocouples or plate thermometers. In France Ed:M.Curtat, Poitiers, editor, *Proceedings of the 6th International Symposium IAFSS*, pages 531–542, 1999.

[25] C. Soize. Maximum entropy approach for modeling random uncertainties in transient elastodynamics. *Journal of Acoustical Society of America*, 5(109):1979–1996, 2001.